scientific reports

Check for updates

OPEN

A Monte Carlo simulation of gamma-ray backscattering from concrete shields coated with nanoparticle layers

Arian Nikrah[1], Payvand Taherparvar[2]✉ & Alireza Sadremomtaz[2]

In recent years, nanocomposite shields have emerged as a promising alternative to conventional lead ones, with rapidly growing applications in medical and industrial sectors. Although the scattering characteristics of nanocomposite shielding materials have been widely investigated, their backscattering behavior remains unexplored in scientific studies. Therefore, obtaining accurate measurements of gamma photon backscattering is essential for evaluating the effectiveness of nanomaterials in radiation shielding. This study investigates the influence of nanoparticles on gamma photon backscattering in low-density polyethylene (LDPE)-based composite radiation shields, using Monte Carlo simulations. Following the validation with available experimental and simulation results, the photon backscattering of LDPE composites doped with W, Ti, Zn, Pb, and Bi particles layered over concrete were analyzed at weight percentages (wt%) of 5%, 10%, 15%, and 20%, and particle sizes ranging from bulk and microscale (10 μm) to nanoscale (100 nm) via the MCNPX code. For comparison purposes, the reflection coefficient (RC) was calculated for 0.1–15 MeV gamma-rays at reflection angles of 92° to 165° and the photon energy spectra were elevated for 0.25, 0.5, and 1 MeV gamma-rays at 135° reflection angle through simulating the ring dosimeters in the proper positions. The results indicate that RC value decreases with increasing the incident gamma energy, reaching its minimum at 15 MeV in all configurations. Besides, the maximum RC (40.18) is observed in gamma energy of 0.1 MeV, in the case of a sample doped with 20% wt of Bi nanoparticles. Moreover, numerical comparisons reveal that reducing particle size enhances the RC, so that nanoscale composites exhibiting a 15–30% higher RC than bulk counterparts at lower energies. Notably, the highest improvement in shielding performance was achieved with 20% Bi nanoparticles at low energies (0.1 MeV), where RC increased by 15% compared to standard concrete. Furthermore, the findings demonstrate that increasing the wt% from 5 to 20 at nanoscale dimensions reduces the number of gamma-photons detected by 25%. Additionally, reducing particle size from bulk case and 10 μm to 100 nm leads to a slight decline in gamma counts (about 8%), attributed to a higher surface-to-volume ratio and increased scattering events. In overall, these findings confirm the effectiveness of nanoparticle composites in enhancing radiation shielding performance and highlight their potential as advanced, lead-free alternatives for medical and industrial applications.

Keywords Backscattering, Nanoparticle, MCNPX, Reflectance coefficients, Gamma spectra

Ionizing radiation can deposits enough energy to ionize organic materials, making them harmful and potentially lethal to living beings[1]. Therefore, various shielding equipment has been developed to protect humans and their surroundings from hazardous radiation effects[2]. Lead and concrete are widely used in radiation shielding applications due to the combination of high atomic number (Z), high density, and strong radiation attenuation coefficients. The electron-rich atomic structures of lead and concrete enhance photon absorption, primarily through the photoelectric effect which is highly dependent on the atomic number (approximately proportional to Z^3), Compton scattering (proportional to Z), and pair production (proportional to Z^2). Photons are fully absorbed in the process of photoelectric absorption and pair production. However, gamma-rays are not entirely absorbed in Compton scattering and coherence scattering, and a portion of the scattered gamma photons may move backward from the surface of a material as the backscattering photons[3–5]. Materials with higher

[1]Department of Physics, University Campus 2, University of Guilan, Rasht, Iran. [2]Department of Physics, Faculty of Sciences, University of Guilan, Rasht, Iran. ✉email: p.taherparvar@guilan.ac.ir; p.taherparvar@gmail.com

atomic numbers are more likely to increase backscattering due to the direct relationship between Compton and coherence scattering with the atomic number. Hence, some studies have been conducted to investigate the effects of backscattered radiation by calculating backscattering gamma-rays and energy distribution of backscattered photons[6–10]. In a recent study, Aydın[7] conducted Monte Carlo simulations to determine the energy distribution of multiply backscattered events resulting from photon interactions with various thicknesses of aluminum, copper, zinc, silver, tin, gold, lead, water, bone, and concrete materials and 0.279, 0.662, 1.25, and 2.1 MeV energy ranges using the Monte Carlo code. As result shows with the increase in the material thickness, the number of backscattered photons with low energies decreases. Therefore, the photoelectric effect is the dominant photon interaction process in the lower energy region[7].

Consequently, understanding backscattered gamma-rays is crucial for minimizing radiation risks to personnel working in medical centers, which often receive less focus. The nature of gamma photon reflection on the surface of a scattering medium depends on the energy and angular distribution of the initial flux[4,9,11–13], which is evaluated by the reflection coefficient (RC) parameter. The RC refers to the ratio of gamma-photons reflected from the surface of a material or from various depths within the material to those incidents on the surface. For practical applications, the RC is also defining the percentage of the incoming dose reflected by a surface at specific angles[14,15]. Al-Affan et al.[16] recently investigated photon backscattering from lead-layered concrete using Monte Carlo simulations via the FLUKA code, covering photon energies between 0.25 and 20 MeV. The RC was computed for various lead thicknesses (0.2 mm to 2 cm) over concrete. By emphasizing the dose reduction potential of thin lead layers, the study determined that a 2 mm thickness of lead as the optimal layer for reducing backscatter doses at low photon energies (< 2.5 MeV). Furthermore, numerical results indicated that RC increases with reflection angle, peaking at 165°, while decreasing with photon energy due to forward scattering effects.

A related study conducted by Qutub investigated the relationship between the RC and the thickness of stainless steel for various incoming photon energies. The work aimed to calculate the saturating thicknesses of stainless steel for various incoming photon energies using the FLUKA Monte Carlo code. The result shows that the number of backscattered events grows with increasing thickness, and the saturation depth of the stainless steel is at a thickness of 2 cm. These findings suggest that stainless steel may be used as a shield for radiation facilities to minimize backscattered photon dose in the incident energy range of less than 2.8 MeV compared to ordinary concretes[17].

However, research on the angular scattering of photons has primarily concentrated on conventional shielding materials and macroscopic protective layers. In the context of nanoparticle doped shields, investigations have been limited to assessment of photon attenuation during transmission[18–21].

Consequently, a comprehensive detailed investigation of gamma-ray backscattering in composites containing nanoparticles and microparticles remains unexplored, especially in terms of new materials and compound incorporating nanoparticles. Hereby, this study seeks to provide backscattering spectra of gamma-ray from irradiation of novel LDPE shields containing nanoparticles by using Monte Carlo N-Particle Extended (MCNPX) codes[22]. For comparison purposes, the RC of LDPE composites containing W, Ti, Zn, Pb, and Bi nano and microparticles with varying concentrations are examined. The evaluations have been expanded for energies ranging from 0.1 to 15 MeV, which is commonly used in photon calculations in the shielding evaluation by ANSI/ANS standards[13].

Materials and methods

Simulation method

This study employs the MCNPX code (version 2.6.0) for simulation purposes. The MCNPX, an extension of the Monte Carlo N-Particle code, is a versatile tool designed for simulating the transport of various particle types, including neutrons, photons, electrons, and coupled neutron/photon/electron interactions[22]. The geometry configuration is implemented in the MCNPX code to assess different backscattering properties. In addition, RC and spectra of backscattered gamma photons were evaluated for samples containing nanoparticles, microparticles, and bulk materials (which are generally larger than the first two in size and often visible to the naked eye). However, in order to doping nano and microparticles into the composite, sample geometry is necessary to discretized into a lattice structure (an MCNPX model was developed using the lattice (LAT) and universe (U) cards to define a cubic matrix uniformly doped with a central spherical filler, representing either a nanoparticle or a microparticle), each nanoparticle is modeled as a sphere and positioned at the center of a unit cell within the meshed geometry. Therefore, samples consist of a cuboid rectangular prism subdivided into N cubes, forming a matrix structure. Perfect spheres are placed at the center of each cube as nano and micro particle, acting as fillers. As the cube dimensions vary, the diameters of the spheres (nano and micro particles) are adjusted accordingly to maintain a uniform filler distribution throughout the matrix. For validation of the simulated sample designed to study nanoparticle backscattering in the composite, the narrow beam setup was utilized. In order to simulate a narrow beam configuration, based on the Beer-Lambert law, a photon point source was placed at a distance of 10 cm from the LDPE/W sample with dimensions of $0.1 \times 100 \times 100$ cm^3 and placed a 0.5 cm spherical detector was place 10cm behind the LDPE/W sample. This study employed the ENDF/B-VI-Release 8 nuclear data evaluation libraries[21]. Consequently, the simulated geometry was validated by comparing the results with the experimental data and the reported data by Alaviani and Tavakoli[23] to ensure that the MCNPX-modeled sample involving nanoparticle-based samples is sufficiently accurate and reliable for use as a nanoparticle-containing radiation shield in this study, Additionally, Simulations involving 60 million particles were executed on an AMD Ryzen 3950X CPU to maintain statistical errors below 1% across all runs. Subsequently, after ensuring the sample's accuracy, A specific geometric configuration, based on previous studies Al-Affan et al.[16], was utilized. The accuracy of this geometric structure was verified using the RC parameter for standard concrete shielding and comparing the obtained results with those from earlier research Al-Affan et

al. and NCRP 151[16,24]. Therefore, Evaluation of the RC parameter was performed following the geometry and simulation protocol from Al-Affan et al.[16], at the first step, incident dose (D_0) was calculated by simulation of a source consisting of a conically diverging photon beam with a radius of 5.65 cm at the surface of the reflective material, yielding an equivalent area of 10×10 cm^2 field size, as shown in Fig. 1. The photon source was positioned 100 cm from the surface of a rectangular parallelepiped water phantom (as a detector). Several smaller dosimeters were simulated within the detector at different depths (1–50 cm) along the central axis. These dosimeters were in rectangular shape and composed of unit density water as a surrogate to tissue-equivalent material. The gamma-ray dose was calculated for each dosimeter inside the phantom, and the maximum dose was identified and considered as the backscattered dose (D_0). The incident photons had energies of 0.1, 0.25 0.5, 0.662, 0.8, 1, 2, 5, 8, 10, and 15 MeV, commonly used in photon calculations according to the ANSI/American National Standard (ANS)[21]. To improve dosimeter efficiency and minimize simulation time, water-based ring dosimeters were positioned at a radius of 1 m inside a vacuum-filled semi-spherical structure. The ring dosimeters were systematically positioned on the sphere's surface to align with the reflection angles to calculate D_b. The reflection angles regarding the incident trajectory, normal to the surface, were taken at 92°, 105°, 120°, 135°, 150°, and 165° based on the Al-affan and et al. and Qutub study[16,17], which shown in Fig. 1. To investigate the backscattering effect in nanometer samples, the RC was calculated using the following relationship:

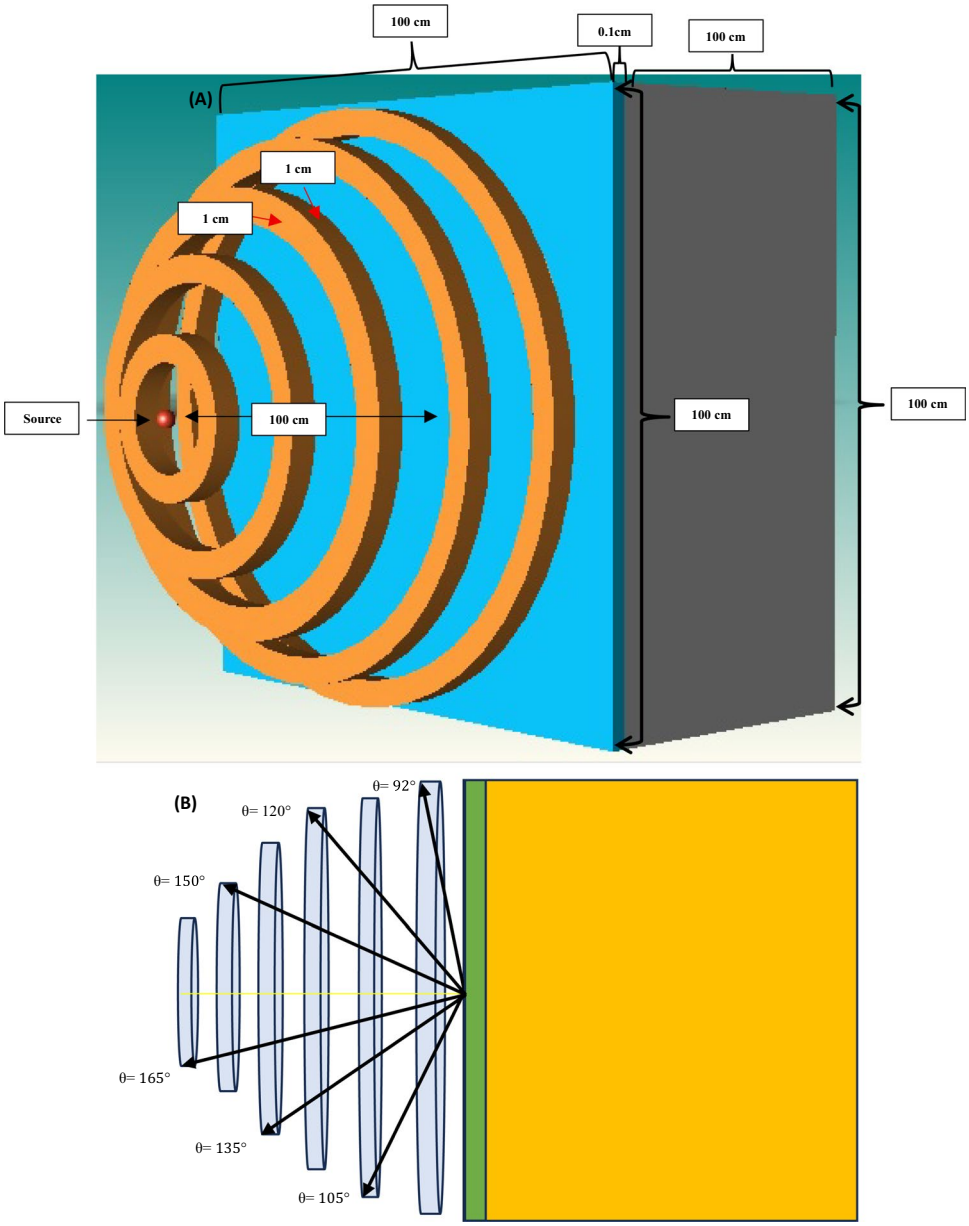

Fig. 1. Geometry simulation of the ring dosimeters to calculate the dose of backscattered photons at reflection angles (**A**) 3D view of simulation geometry, (**B**) 2D view of simulation geometry.

$$RC = \frac{D_b}{D_0} \quad (1)$$

where D_0 represents the incident dose and D_b denotes the backscattered dose[16,17].The ring dosimeters were 1 cm thick (between the inner and outer circles) and 1 cm in height. Tally *F8 is used to investigate the transmitted energy of a particle through a cell (as the input to calculate D_0 and D_b) in the MCNPX code using the library of Evaluated Nuclear Data Files (ENDF)/B-VI-Released 8.

Therefore, to verify the simulation geometry and simulation protocol, a concrete sample with 100 cm thickness located in front of water detector after calculating D_0 to evaluate D_b, based on the investigated energies (0.5 MeV) and concrete geometry of the Qutub[17] and Al-affan et al.[16]. The results were compared with the NCRP 151[24], and the findings were validated against the data from the research conducted by Al-affan et al.[16].

Subsequently, the F4 tally is applied to measure the transmitted gamma-ray flux, which is essential for evaluating the spectra of backscattered gamma photons[7] and linear attenuation coefficient (μ) for validation purpose[25] using the following relationship:

$$I = I_0 \exp(-\mu x) \quad (2)$$

where I and I_0 are transmitted and incident gamma-ray intensity, respectively.

Besides, employing the configuration presented in Fig. 1, a backscatter angle of 135° (as established in prior studies by Al-affan and Qutab[16,17]) and a gamma energy of 0.25, 0.5, and 1 MeV were adopted to evaluate the spectra of gamma-rays in LDPE-based composites containing 5–20 wt% tungsten nanoparticles. The number of 60 million photons were generated to get a statistical uncertainty of less than 1% all situations. In Figs. 3, 4 and 5 concerning the RC value, the vertical error bars provided indicate one standard error of the mean (calculated as the standard deviation of the mean divided by the square root of the total number of photons). The sample code used to design and evaluate the geometry under study for the validation simulations is also presented in the "Supplementary information" section.

Results and discussion

Validation

The simulation geometry was evaluated and validated in two stages based on prior research to investigate the effect of the RC and spectra of gamma-ray backscattered photons for LDPE shields containing W, Ti, Zn, Pb, and Bi particles.

Firstly, the lattice (LAT) and universe (U) cards in the MCNPX code were utilized to define a polymer matrix homogeneously doped with a nanoparticle and microparticle filler, to ensure the correct arrangement of nanoparticles and microparticles within the cubic LDPE matrix, the linear attenuation coefficient (μ) of LDPE composites doped with varying percentages of W particles were calculated using the MCNPX code for gamma-photons at 1.25 MeV. The simulation geometry consisted of a a point source emitting monoenergetic gamma-photons was placed 100 cm from a $100 \times 100 \times 0.1$ cm LDPE/W composite, A spherical detector with a 0.5 cm radius was positioned behind the sample to measure the transmitted flux using the F4 tally[25]. The μ were derived from the ratio of the flux with and without the sample, accounting for the sample's density and thickness. This approach ensures accurate modeling of photon interactions within the composite material, crucial for designing effective radiation shields. the results of the μ for the LDPE/W samples were compared with the experimental findings from Kim et al.[26], Azeez et al.[27], and the research conducted by Alaviani and Tavakoli[25]. The results are presented in Table 1.

According to Table 1, the highest discrepancy from the experimental results at the micrometer scale is 5.93% for all wt% of W, while the most significant difference from the simulation results is 5.2%. Additionally, at the nanometer scale, the maximum deviation from the experimental results is 1.47% for all wt% of the material, compared to a discrepancy of 4.6% from the simulation. Therefore, based on the results presented in Table 1 and the substantial agreement between this study and previous research, the geometry can be considered highly reliable for investigating shields containing nanoparticles and microparticles.

Secondly, to validate the accuracy of simulated geometry, the RC of concrete shield was evaluated by water dosimeter modeled as a rectangular slab with a thickness of 100 cm and a point source was positioned 100 cm

Composition nano	Exp (Kim)	This study	Diff (%)	Alavidani	This study	Diff (%)
LDPE: 7.5wt% W	0.061	0.06	1.47	0.063	0.06	4.6
LDPE: 15wt% W	0.067	0.0667	0.33	0.068	0.0667	1.79
Composition micro	**Exp (Azeez)**	**This study**	**Diff (%)**	**Alavidani**	**This study**	**Diff (%)**
LDPE 30wt% W	0.13	0.13	2.47	0.12	0.13	5.2
LDPE: 50wt% W	0.1	0.1	3.66	0.09	0.1	2.23
LDPE: 70wt% W	0.2	0.19	5.93	0.19	0.19	0.1
LDPE: 80wt% W	0.27	0.26	2.41	0.26	0.26	2.0

Table 1. MCNP and experimental (Exp) data comparison for μ (cm^{-1}) of LDPE/W composites for W particle sizes of 300 nm (Kim et al.[26]), 6 μm (Azeez et al.[27]), 300 nm and 6 μm (Alaviani and Tavakoli[25]).

from the front face of a dosimeter to calculate D_0. Subsequently, to obtain the shielded dose rate (D_b), the simulation was repeated with the shield in place and by adding water ring detectors, as shown in Fig. 1[16].

The results, as shown in Fig. 2, indicate a good agreement between the simulation data and previous research. The data deviation is less than 1%.

RC of concrete sample layered with LDPE containing various wt% of nanoparticles

The RC values for 92°, 105°, 120°, 135°, 150°, and 165° reflection angles of the LDPE, thickness of 0.1 cm, containing 5%, 10%, 15%, and 20% of W, Ti, Zn, Pb, and Bi nanoparticles were performed by using MCNPX code for energies of 0.1, 0.25, 0.5, 0.662, 0.8, 1, 2, 5, 8, 10, and 15 MeV. The LDPE was lined with 100 cm concrete. The results of the variations in RC as a function of gamma-ray energy have been presented in Tables 2, 3, 4, 5 and 6.

Tables 2, 3, 4, 5 and 6 show that the RC gradually decreases due to the increase in incident gamma-photons energy from 0.1 to 15 MeV, and the corresponding reduction in the shielding effectiveness of the material; the RC increases as the absorption cross-section of the reflecting sample increases, roughly in proportion to Z^2.

Moreover, the results show that low-energy gamma-rays contribute more significantly to RC than those at higher energies. This can be attributed to their lower penetration depth and the than of multiple interactions within the samples. At higher energies, the influence of Compton scattering diminishes, while gamma photon transmission through the shield is enhanced. Pair production becomes the dominant photon-matter interaction, consequently causing a sharp decrease in the RC. This behavior implies a reduction in the number of backscattered gamma photons, despite the diminished shielding capacity of the sample. Furthermore, Tables 2 3, 4, 5 and 6 indicate that a higher nanoparticle wt% results in a gradual enhancement of RC. Notably, the samples containing 20 wt% nanoparticles exhibit the highest RC within the 2–15 MeV energy range. Additionally, as shown in ,Tables 2 3, 4, 5 and 6, regardless of the increase in wt% of nanoparticles, a rise in the reflection angle from 92 to 165° results in a corresponding growth in the RC. Moreover, the data in Tables 2, 3, 4, 5 and 6 indicate a slight increase in the RC as the wt% of W, Ti, Zn, Pb, and Bi in the LDPE composite increases from 5 to 20%. The probabilities of scattering and absorption are inversely related. It is known theoretically that a material exhibits better shielding properties when it has higher RC values. Therefore, increasing wt% of W, Ti, Zn, Pb, and Bi nanoparticles in LDPE samples results in better shielding properties.

The effect of reducing particle size on RC of concrete sample layered with LDPE compound

To evaluate the effects of particle size on RC of LDPE samples doped with W, Ti, Zn, Pb, and Bi, two wt% (5% and 20%) and three particle sizes (100 nm, 10 μm and bulk) the reflection angle of 135° of W, and Bi particles were analyzed using the geometry depicted in Fig. 1.

Figure 3 presents the calculated RC values relative to the incident gamma-ray energy. The results show that for all particle sizes of W, Ti, Zn, Pb, and Bi-doped into LDPE composite, an increase in wt% from 5 to 20% wt of particles leads to a corresponding increase in the RC. The highest RC occurs at lower energies because of the sample ability to absorb low-energy gamma-rays. Therefore, the RC increases for all particle sizes at this energy range. At higher energies, the RC decreases because of the diminished capacity of the shield to absorb gamma-rays. Furthermore, the RC increases as the particle size decreases from bulk to 100 nm. This

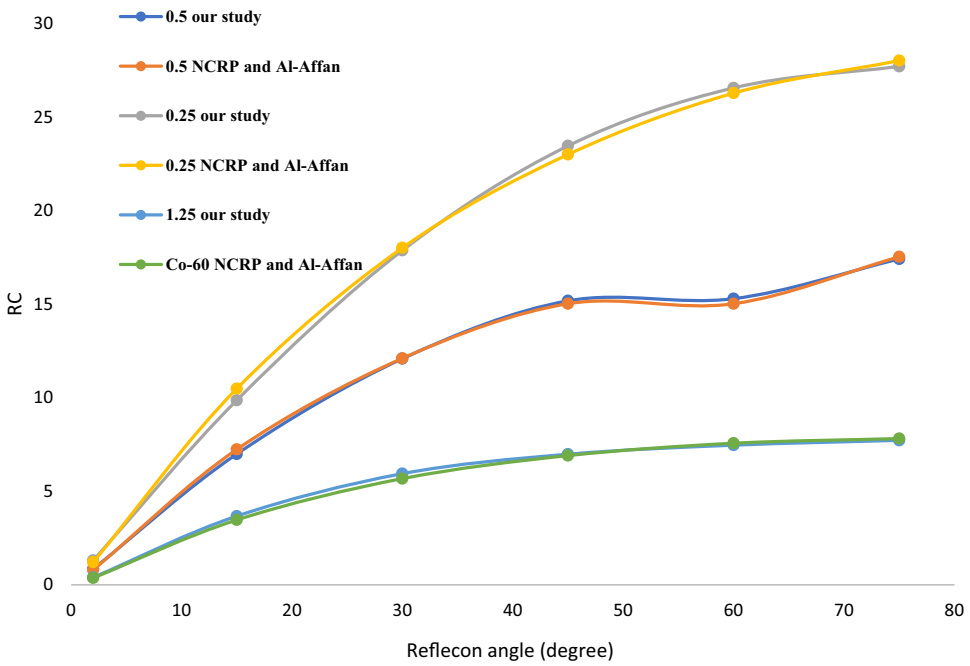

Fig. 2. Comparison between the simulation results from this study with the data reported by Al-Affan and NCRP 151[16,24].

		Energy (MeV)										
	The angle of reflection (degrees)	0.1	0.25	0.5	0.662	0.8	1	2	5	8	10	15
Bi 5%wt	165°	37.02	27.60	17.12	13.19	11.03	9.40	4.58	2.82	2.49	2.38	2.11
	150°	34.65	26.23	16.24	13.14	10.77	8.94	4.54	2.78	2.45	2.33	1.98
	135°	29.30	23.48	14.94	11.60	10.02	8.02	4.21	2.44	2.00	1.95	1.70
	120°	22.77	18.11	12.14	9.44	8.29	6.74	3.49	1.97	1.57	1.48	1.34
	105°	12.05	8.98	6.36	5.19	4.61	3.83	1.87	1.09	0.86	0.77	0.66
	92°	1.65	0.96	0.63	0.49	0.46	0.37	0.21	0.11	0.09	0.07	0.06
		Energy (MeV)										
	The angle of reflection (degrees)	0.1	0.25	0.5	0.662	0.8	1	2	5	8	10	15
Bi 10%wt	165°	38.68	27.91	17.69	13.44	11.29	9.65	4.61	2.85	2.54	2.39	2.12
	150°	36.74	26.81	16.50	13.18	10.92	9.16	4.61	2.80	2.46	2.33	1.99
	135°	29.98	23.63	15.14	11.88	10.12	8.20	4.27	2.42	2.02	1.96	1.70
	120°	23.06	18.37	12.16	9.61	8.44	6.91	3.57	1.98	1.57	1.50	1.33
	105°	12.3	9.21	6.77	5.43	4.73	3.94	2.12	1.10	0.86	0.78	0.67
	92°	1.77	0.98	0.73	0.55	0.49	0.40	0.22	0.11	0.09	0.08	0.07
		Energy (MeV)										
	The angle of reflection (degrees)	0.1	0.25	0.5	0.662	0.8	1	2	5	8	10	15
Bi 15%wt	165°	39.42	28.23	18.20	13.79	11.49	9.83	4.78	2.87	2.56	2.41	2.12
	150°	37.84	26.97	17.22	13.22	11.11	9.49	4.70	2.85	2.51	2.33	2.00
	135°	30.53	23.76	15.24	12.15	10.27	8.51	4.30	2.48	2.05	1.97	1.74
	120°	23.71	18.43	12.22	9.79	8.68	7.06	3.60	1.98	1.60	1.53	1.36
	105°	11.97	9.60	6.84	9.83	4.80	4.09	2.16	1.13	0.87	0.80	0.67
	92°	1.92	1.01	0.80	0.63	0.58	0.48	0.25	0.12	0.09	0.08	0.07
		Energy (MeV)										
	The angle of reflection (degrees)	0.1	0.25	0.5	0.662	0.8	1	2	5	8	10	15
Bi 20%wt	165°	40.18	28.63	18.27	13.95	11.80	10.42	4.81	2.89	2.65	2.42	2.13
	150°	38.67	27.29	17.70	13.25	11.42	9.99	4.75	2.88	2.55	2.37	2.00
	135°	31.73	23.88	15.27	12.27	10.39	8.71	4.33	2.52	2.09	1.98	1.74
	120°	24.61	18.67	12.25	9.91	8.80	7.86	3.61	2.00	1.68	1.55	1.36
	105°	12.11	9.77	6.86	5.76	4.98	4.93	2.17	1.14	0.87	0.81	0.68
	92°	2.08	1.06	0.88	0.66	0.61	0.58	0.26	0.13	0.09	0.08	0.07

Table 2. LDPE incorporating different wt% of Bi nanoparticles.

indicates that decreasing the particle size of W, Ti, Zn, Pb, and Bi particles to 100 nm enhances both coherent and Compton scattering of gamma-rays when interacting with the sample shield in smaller particle sizes. As gamma energy increases, the Compton scattering effect weakens, and pair production becomes the dominant interaction, resulting in a pronounced decrease in the RC. In contrast, as shown in Fig. 3, reducing the particle size from bulk and 10 μm to 100 nm still improves the RC of the samples. Therefore, the maximum RC in the 2–15 MeV energy range is observed in LDPE samples containing 20 wt% of 100 nm particles. As a result of the size reduction, the RC increases, with the highest RC observed at dimensions of 100 nm, while the lowest RC is seen in the bulk dimensions. Furthermore, as the wt% of particles in the LDPE composite increases, the RC increases in all dimensions. The most significant increases in RC are observed at 20% wt in 100 nm of particle radius.

The normalized RC of LDPE sample containing various wt% of nanoparticles

To investigate the effect of adding an LDPE sample containing 5–20% of W, Ti, Zn, Pb, and Bi nanoparticles to the ordinary concrete on RC value and evaluate whether incorporating the LDPE sample changes the effectiveness of the shielding configuration, the results from Tables 2, 3, 4 and 5 in the 0.1–15 MeV energy range were normalized to the results of ordinary concrete, as shown in Fig. 4.

According to Fig. 4, the absorption in the LDPE sample containing W, Ti, Zn, Pb, and Bi nanoparticles is more significant compared to ordinary concrete. At lower energies, these results highlight the radiation shielding efficacy of the nanoparticle composite. Consequently, the LDPE sample containing 20 wt% Bi nanoparticles demonstrated the highest normalized RC, showing an 18% improvement compared to the undoped samples. This is influenced by the high shielding properties of the nanoparticle-containing composite. As the energy increases, the RC enhancement in nanoparticle-containing samples gradually diminishes, such that at higher energies, these samples exhibit a lower normalized RC than ordinary concrete (the lowest value corresponds to the LDPE sample doped with 5 wt% Zn nanoparticles, showing a 6% reduction). With an increase in the nanoparticle wt%, the RC rises across all nanoparticle-containing compositions at all energy levels. The lowest

	Energy (MeV)										
The angle of reflection (degrees)	0.1	0.25	0.5	0.662	0.8	1	2	5	8	10	15
165°	38.24	28.03	17.05	13.47	11.23	9.25	4.63	2.86	2.52	2.27	2.10
150°	35.53	26.37	16.72	13.04	11.08	8.97	4.55	2.73	2.35	2.29	1.95
135°	29.63	23.31	15.13	11.83	9.98	8.15	4.20	2.45	2.03	1.93	1.69
120°	22.38	18.04	12.46	9.70	8.18	6.68	3.47	1.88	1.62	1.54	1.32
105°	12.21	8.76	6.30	5.54	4.52	3.81	2.03	1.04	0.85	0.77	0.66
92°	1.72	0.81	0.74	0.61	0.48	0.39	0.22	0.10	0.09	0.09	0.06

		Energy (MeV)										
	The angle of reflection (degrees)	0.1	0.25	0.5	0.662	0.8	1	2	5	8	10	15
Pb10%wt	165°	38.86	28.11	17.78	13.76	11.43	9.55	4.66	2.91	2.56	2.33	2.11
	150°	35.88	26.67	17.08	13.17	11.22	9.14	4.57	2.72	2.37	2.19	1.95
	135°	30.72	23.49	16.16	12.02	10.14	8.52	4.22	2.47	2.05	1.99	1.73
	120°	23.55	18.34	13.16	9.78	8.23	7.09	3.49	1.91	1.59	1.48	1.25
	105°	12.39	9.06	6.50	5.34	4.61	4.17	2.05	1.05	0.87	0.77	0.66
	92°	1.83	0.88	0.78	0.62	0.52	0.44	0.24	0.11	0.09	0.09	0.07

	The angle of reflection (degrees)	Energy (MeV)										
		0.1	0.25	0.5	0.662	0.8	1	2	5	8	10	15
Pb 15%wt	165°	39.03	28.28	18.4	13.89	11.55	9.88	4.83	2.92	2.60	2.35	2.11
	150°	36.62	27.06	17.9	13.39	11.35	9.38	4.67	2.73	2.38	2.25	1.97
	135°	31.80	23.75	16.98	12.19	10.22	8.96	4.25	2.48	2.11	2.00	1.74
	120°	24.22	18.42	13.89	9.67	8.31	7.63	3.55	1.92	1.60	1.48	1.25
	105°	12.69	9.16	6.76	5.43	4.63	4.59	2.10	1.06	0.88	0.83	0.67
	92°	1.88	0.92	0.82	0.66	0.55	0.49	0.27	0.11	0.10	0.10	0.07

		Energy (MeV)										
	The angle of reflection (degrees)	0.1	0.25	0.5	0.662	0.8	1	2	5	8	10	15
Pb 20%wt	165°	39.95	28.52	19.01	14.07	11.97	10.06	4.90	3.00	2.60	2.35	2.18
	150°	37.38	27.41	18.34	13.52	11.43	9.93	4.65	2.76	2.40	2.26	1.99
	135°	32.46	24.15	17.30	12.29	10.38	9.13	4.25	2.47	2.15	2.02	1.73
	120°	25.39	18.65	14.09	9.53	8.48	8.02	3.58	1.95	1.63	1.55	1.31
	105°	13.32	9.44	7.18	5.56	4.76	4.90	2.10	1.14	0.88	0.83	0.68
	92°	2.03	0.98	0.87	0.70	0.64	0.54	0.31	0.12	0.11	0.10	0.07

Table 3. LDPE incorporating different wt% of Pb nanoparticles.

RC is observed at 5% wt for all LDPE samples doped with nanoparticles, while as the wt% increases to 20%, the RC also increases, with the highest RC observed at 20% wt.

The particle size redction on normalized RC of the LDPE compound

To assess the effects of particle size on the RC of LDPE samples doped with Pb, W, Bi, Zn, and Ti compared to ordinary concrete, two wt% (5% and 20%), three particle sizes (100 nm, 10 μm, and bulk), and a reflection angle of 135° were analyzed, following the geometry shown in Fig. 2. Figure 5 displays the calculated RC values normalized to the ordinary concrete in terms of incident photon energy.

According to Fig. 5, the comparison reveals that the highest normalized RC difference occurs at low energies relative to ordinary concrete, and this difference gradually decreases as the energy increases. Finally, at 15 MeV, the RC difference reaches its minimum across all wt% and particle sizes. The lowest normalized RC is observed in the LDPE sample containing 5 wt% bulk Zn, with a 6% reduction to ordinary concrete. Furthermore, as shown in Fig. 5, reducing particle size from bulk to the nanoscale increases the RC, indicating enhanced shielding properties of the LDPE composite containing Pb, W, Bi, Zn, and Ti particles. The LDPE containing 20 wt% W nanoparticles showing the highest improvement (27%) in normalized RC compared to concrete. Additionally, a gradual improvement in RC is observed as the wt% of all Pb, W, Bi, Zn, and Ti particles in the composite increases from 5 to 20% across all particle sizes. When comparing LDPE composites with Pb, W, Bi, Zn, and Ti particles to ordinary concrete, this enhancement in the RC difference becomes more pronounced as the particle size is reduced progressively from bulk to microscale and then to nanoscale dimensions. The highest RC is found at 100 nm with a *20% wt of nanoparticles within the LDPE.*

Backscattered gamma photon spectra of LDPE samples doped with various wt% of W nanoparticles

The spectra of photons backscattered, considering 0.5 MeV gamma-rays for LDPE-based composites doping with nanoparticles of W (5–20 wt%), were modeled and evaluated using the MCNP code at a 135° backscattering

	Energy (MeV)										
The angle of reflection (degrees)	0.1	0.25	0.5	0.662	0.8	1	2	5	8	10	15
165°	36.22	27.76	18.10	12.95	10.57	9.58	5.34	2.90	2.53	2.21	2.05
150°	33.22	26.64	16.85	12.81	10.61	8.10	4.65	2.73	2.40	2.24	1.93
135°	28.38	22.88	15.17	11.98	10.07	7.98	4.14	2.46	1.99	2.00	1.70
120°	20.74	17.98	11.59	9.11	8.05	6.53	3.41	1.90	1.62	1.54	1.28
105°	9.96	9.11	6.98	5.26	4.18	3.90	2.00	0.99	0.89	0.82	0.66
92°	1.23	0.88	0.86	0.59	0.56	0.42	0.16	0.13	0.11	0.09	0.07
		Energy (MeV)										
	The angle of reflection (degrees)	0.1	0.25	0.5	0.662	0.8	1	2	5	8	10	15
Zn 10%wt	165°	36.72	27.81	18.70	13.01	10.78	9.80	5.35	2.89	2.54	2.21	2.08
	150°	33.62	26.79	16.88	12.91	10.74	8.63	4.54	2.73	2.40	2.26	1.95
	135°	28.88	23.27	16.30	12.03	10.11	8.45	4.31	2.47	2.05	2.02	1.70
	120°	21.34	18.11	11.79	9.35	8.14	6.74	3.54	1.92	1.63	1.56	1.31
	105°	10.16	9.25	7.07	5.63	4.37	4.02	2.03	1.04	0.89	0.83	0.67
	92°	1.33	0.89	0.87	0.59	0.58	0.44	0.17	0.13	0.11	0.09	0.07
		Energy (MeV)										
	The angle of reflection (degrees)	0.1	0.25	0.5	0.662	0.8	1	2	5	8	10	15
Zn 15%wt	165°	37.04	27.89	19.20	13.49	11.12	10.16	5.38	2.90	2.54	2.22	2.09
	150°	33.98	26.83	17.20	13.01	10.93	9.31	4.55	2.74	2.42	2.29	2.00
	135°	29.45	23.47	16.91	12.08	10.24	8.83	4.38	2.48	2.09	2.02	1.70
	120°	21.78	18.32	12.46	9.68	8.19	7.11	3.61	1.93	1.65	1.56	1.29
	105°	10.68	9.37	7.33	5.67	4.52	4.19	2.13	1.13	0.90	0.83	0.68
	92°	1.66	0.93	0.88	0.62	0.58	0.47	0.19	0.13	0.11	0.09	0.07
		Energy (MeV)										
	The angle of reflection (degrees)	0.1	0.25	0.5	0.662	0.8	1	2	5	8	10	15
Zn 20%wt	165°	37.67	27.98	19.87	13.78	11.54	10.54	5.44	2.91	2.56	2.25	2.11
	150°	34.10	26.96	17.98	13.19	10.98	9.82	5.30	2.74	2.44	2.30	2.01
	135°	29.78	23.64	17.12	12.15	10.34	9.37	4.79	2.49	2.11	2.03	1.71
	120°	22.22	18.54	12.60	9.74	8.25	7.77	3.94	1.94	1.67	1.57	1.30
	105°	10.84	9.41	7.62	5.71	4.74	4.32	2.36	1.16	0.91	0.83	0.70
	92°	1.83	0.96	0.88	0.64	0.61	0.51	0.21	0.14	0.12	0.09	0.07

Table 4. LDPE incorporating different wt% of Zn nanoparticles.

angle. Figure 6 presents the impact of varying nanoparticle wt% on the backscattered gamma photons spectra of LDPE doped with W nanoparticle samples.

The results in Fig. 6 indicate that, the spectra of gamma photons backscattered from both concrete and concrete layered with LDPE composite exhibit a prominent peak near 0.2 MeV. This peak, caused by Compton scattering alone, referred to as the backscattering peak. Ordinary concrete exhibited the highest peak in the spectrum of backscattered photons. When LDPE composites containing 5 to 20 wt% of W nanoparticles were placed alongside the concrete sample, this led to a decrease in the gamma photons backscattered spectra, which is more pronounced as the W nanoparticle wt% increases. Such reduction behavior is primarily driven by the increased gamma photon absorption cross-section of W at higher wt%, which significantly raises the probability of photon-matter interactions and reduces the intensity of the backscattered photons. Therefore, while the minimum photon count is recorded for the LDPE sample with 20 wt% nanoparticles, the maximum one is observed for the LDPE sample with 5 wt% nanoparticles, which highlights the role of the Compton interactions for peak occurrence in the backscattered photons spectra.

Backscattered gamma photon spectra of LDPE samples doped with W particles of various sizes

Figure 7 compares the spectra of photons backscattered at 135° from LDPE composites containing W particles of three different sizes (bulk, 10 μm, and 100 nm) for 0.5 MeV gamma-rays with the corresponding spectrum in the case of ordinary concrete.

As shown in Fig. 7, with increasing energy, a pronounced peak of gamma counts from backscattering photons at approximately 0.2 MeV is obvious. This peak is solely due to Compton-scattered gamma photons from samples. The ordinary concrete sample produces the most significant peak in the spectrum of backscattered gamma photons. When LDPE composites containing 20 wt% W particles (bulk, 10 μm, and 100 nm) are layered on concrete, a reduction in gamma photon counts is observed, which is more pronounced as the size of W particles in the LDPE matrix decreases. While the smallest reduction occurred for LDPE samples containing bulk-sized W particles, it becomes more significant for samples with 10 μm particles, reaching its greatest value in samples

The angle of reflection (degrees)	Energy (MeV)										
	0.1	0.25	0.5	0.662	0.8	1	2	5	8	10	15
165°	36.83	27.19	17.13	13.54	11.74	9.20	4.71	2.95	2.55	2.40	2.09
150°	33.47	26.11	16.50	13.07	10.96	8.90	4.57	2.79	2.40	2.31	1.97
135°	28.98	23.21	15.12	11.75	10.04	8.18	4.38	2.45	2.11	1.98	1.72
120°	20.80	18.16	11.56	9.48	8.33	6.78	3.50	1.93	1.61	1.51	1.27
105°	10.46	8.50	6.36	5.07	4.45	3.75	2.05	1.09	0.88	0.83	0.67
92°	1.19	1.03	0.69	0.53	0.52	0.45	0.25	0.12	0.09	0.08	0.06

	The angle of reflection (degrees)	Energy (MeV)										
		0.1	0.25	0.5	0.662	0.8	1	2	5	8	10	15
W 10%wt	**165°**	37.20	27.92	17.31	13.70	11.86	9.42	4.75	2.99	2.59	2.43	2.10
	150°	33.64	26.20	16.62	13.21	11.07	8.93	4.71	2.90	2.48	2.32	1.97
	135°	29.07	23.46	16.15	11.93	10.12	8.30	5.12	2.46	2.13	1.98	1.74
	120°	21.41	18.60	11.89	9.66	8.20	7.02	3.51	1.95	1.61	1.53	1.27
	105°	10.55	9.33	6.58	5.32	4.64	3.98	2.05	1.11	0.89	0.83	0.68
	92°	1.29	1.04	0.71	0.59	0.57	0.48	0.26	0.12	0.10	0.08	0.06

	The angle of reflection (degrees)	Energy (MeV)										
		0.1	0.25	0.5	0.662	0.8	1	2	5	8	10	15
W 15%wt	**165°**	38.68	27.86	17.7	13.83	12.05	9.66	4.86	3.05	2.60	2.44	2.11
	150°	34.12	26.53	1.66	13.48	11.17	9.03	4.72	3.03	2.50	2.31	1.97
	135°	29.83	23.71	17.03	12.05	10.26	8.14	5.35	2.48	2.16	2.00	1.74
	120°	22.33	18.79	12.08	9.75	8.21	7.20	3.72	1.97	1.62	1.54	1.28
	105°	11.40	9.34	6.76	5.56	4.70	4.06	2.06	1.14	0.89	0.84	0.68
	92°	1.33	1.05	0.77	0.63	0.60	0.55	0.27	0.13	0.10	0.08	0.07

	The angle of reflection (degrees)	Energy (MeV)										
		0.1	0.25	0.5	0.662	0.8	1	2	5	8	10	15
W 20%wt	**165°**	39.80	28.06	18.10	14.23	12.18	10.16	4.90	3.12	2.63	2.44	2.13
	150°	35.31	26.82	16.70	13.58	11.33	9.14	4.85	3.21	2.53	2.33	1.97
	135°	29.83	23.94	17.32	12.25	10.32	8.42	5.41	2.54	2.21	2.04	1.75
	120°	22.92	18.97	12.17	9.94	8.28	7.73	3.84	1.98	1.64	1.55	1.30
	105°	11.89	9.83	7.22	5.76	4.82	4.21	2.14	1.18	0.90	0.84	0.69
	92°	1.39	1.10	0.87	0.69	0.62	0.58	0.28	0.14	0.10	0.08	0.07

Table 5. LDPE incorporating different wt% of W nanoparticles.

with 10 nm particles. Hence, the LDPE containing W nanoparticles exhibits the lowest gamma photon counts for all samples. This reduction effect is attributed to a decrease in the Compton scattering probability which is primarily due to the higher surface-area-to-volume ratio and greater absorption ability of W nanoparticles.

Conclusions

This study investigated a novel nanocomposite-based radiation shielding approach to evaluate the effectiveness and backscattering performance of lead-free, nano-doped composite shields. Initially, a two-step process was conducted to validate the accuracy of simulation geometry. The μ of LDPE/W samples with 300 nm and 6 μm particle sizes was compared with experimental data and previous studies, to ensure the proper configuration of the LDPE-based lattice model incorporating spherical nano- and microparticles. Also, to investigate the RC value, a ring dosimeter was incorporated into the geometry, and a concrete sample with a 100 cm thickness was simulated. The results were compared with NCRP 151 data and previous studies, showing a deviation less than 1%. Subsequently, the simulations were performed to obtain and compare RC values for 0.1, 0.25 0.5, 0.662, 0.8, 1, 2, 5, 8, 10, and 15 MeV gamma-rays backscattered from LDPE samples doped with 5%, 10%, 15%, and 20% wt of Pb, W, Bi, Zn, and Ti nanoscale (100 nm), microscale (10 μm) and bulk-sized particles using a fine lattice geometry in the MCNPX code. Additionally, to analyze backscattering through reflection coefficients, a circular ring dosimeter was placed at reflection angles of 92°, 105°, 120°, 135°, 150°, and 165°.

The obtained results show that as the energy increases, the RC of Pb, W, Bi, Zn, and Ti shields gradually decreases, primarily due to the decreasing in probability of Compton scattering at higher energies, reaching its minimum at 15 MeV for all nanoparticle wt%. Here, the LDPE sample containing 20 wt% of Bi nanoparticles shows the highest RC, due to its high atomic number compared to other examined materials. Also, the RC values were analyzed under varying particle sizes and densities to evaluate the impact of adding an LDPE layer doped with Pb, W, Bi, Zn, and Ti to concrete shield, compared to ordinary concrete alone. This suggests that at low photon energies (up to ~ 1 MeV), nanoparticle-based shielding may result in a slight increase in RC (less than 10%) compared to concrete shield, because of the higher photoelectric absorption. Moreover, the lowest overall backscattered gamma counts at 135° angle were obtained for 20 wt% of W nanoparticles, which can be

	Energy (MeV)										
The angle of reflection (degrees)	0.1	0.25	0.5	0.662	0.8	1	2	5	8	10	15
165°	35.68	26.64	17.23	13.46	11.27	9.23	4.76	2.86	2.57	2.37	2.06
150°	32.89	25.26	16.88	13.07	11.07	9.00	4.74	2.69	2.42	2.17	1.97
135°	28.17	23.08	15.08	11.82	9.76	8.14	4.28	2.72	2.12	1.93	1.72
120°	20.38	17.54	11.76	9.57	8.01	6.77	3.65	2.00	1.66	1.47	1.27
105°	11.20	10.14	6.90	5.36	4.42	4.10	2.10	1.10	0.89	0.77	0.70
92°	1.31	0.89	0.65	0.73	0.57	0.43	0.16	0.13	0.10	0.08	0.08

		Energy (MeV)										
	The angle of reflection (degrees)	0.1	0.25	0.5	0.662	0.8	1	2	5	8	10	15
Ti 10%wt	165°	35.88	26.89	17.56	13.66	11.43	9.28	4.79	2.88	2.58	2.43	2.12
	150°	33.15	25.58	17.01	13.29	11.22	9.05	4.75	2.72	2.44	2.18	1.99
	135°	28.64	23.20	15.18	11.91	9.78	8.19	4.29	2.76	2.19	1.93	1.75
	120°	20.65	17.74	12.22	9.67	8.07	6.81	3.71	2.04	1.69	1.50	1.30
	105°	11.87	10.28	6.90	5.42	4.47	4.11	2.22	1.11	0.91	0.81	0.70
	92°	1.32	0.92	0.69	0.74	0.60	0.47	0.16	0.13	0.10	0.08	0.08

		Energy (MeV)										
	The angle of reflection (degrees)	0.1	0.25	0.5	0.662	0.8	1	2	5	8	10	15
Ti 15%wt	165°	36.39	27.06	17.69	13.84	11.50	9.39	4.90	2.89	2.61	2.43	2.12
	150°	33.73	25.76	17.33	13.47	11.32	9.11	4.77	2.74	2.45	2.19	2.05
	135°	28.86	23.51	15.89	12.04	9.81	8.22	4.32	2.80	2.21	2.03	1.78
	120°	20.77	17.98	12.70	9.75	8.19	6.87	3.72	2.11	1.75	1.52	1.30
	105°	11.08	10.35	6.94	5.57	4.56	0.42	2.24	1.11	0.92	0.82	0.72
	92°	1.39	0.95	0.73	0.75	0.62	0.49	0.17	0.13	0.10	0.09	0.08

		Energy (MeV)										
	The angle of reflection (degrees)	0.1	0.25	0.5	0.662	0.8	1	2	5	8	10	15
Ti 20%wt	165°	36.89	27.23	17.89	13.93	11.68	9.44	4.96	2.90	2.64	2.44	2.17
	150°	34.08	25.94	17.72	13.59	11.41	9.13	4.78	2.75	2.47	2.25	2.07
	135°	29.10	23.61	16.14	12.14	9.99	8.92	4.41	2.82	2.23	2.05	1.79
	120°	21.24	18.28	13.16	9.83	8.34	7.13	3.76	2.28	1.87	1.57	1.33
	105°	11.70	10.55	7.28	5.60	4.60	4.32	2.28	1.12	0.94	0.83	0.72
	92°	1.50	1.01	0.76	0.76	0.63	0.51	0.19	0.14	0.10	0.10	0.08

Table 6. LDPE incorporating different wt% of Ti nanoparticles.

attributed to their greater photon absorption cross-sections, leading to more efficient gamma absorption. While the reduction in particle size leads to an increase in the RC, potentially improving the shielding performance, it simultaneously causes a reduction in the overall gamma counts exiting the material. This dual effect underscores the importance of optimizing both the particle size and the particle wt% in the composite design. Since smaller particles not only enhance the reflective properties but also contribute to a lower backscattered gamma count, employing nanocomposite materials with higher percentages of nanoparticles appears more effective for radiation shielding applications.

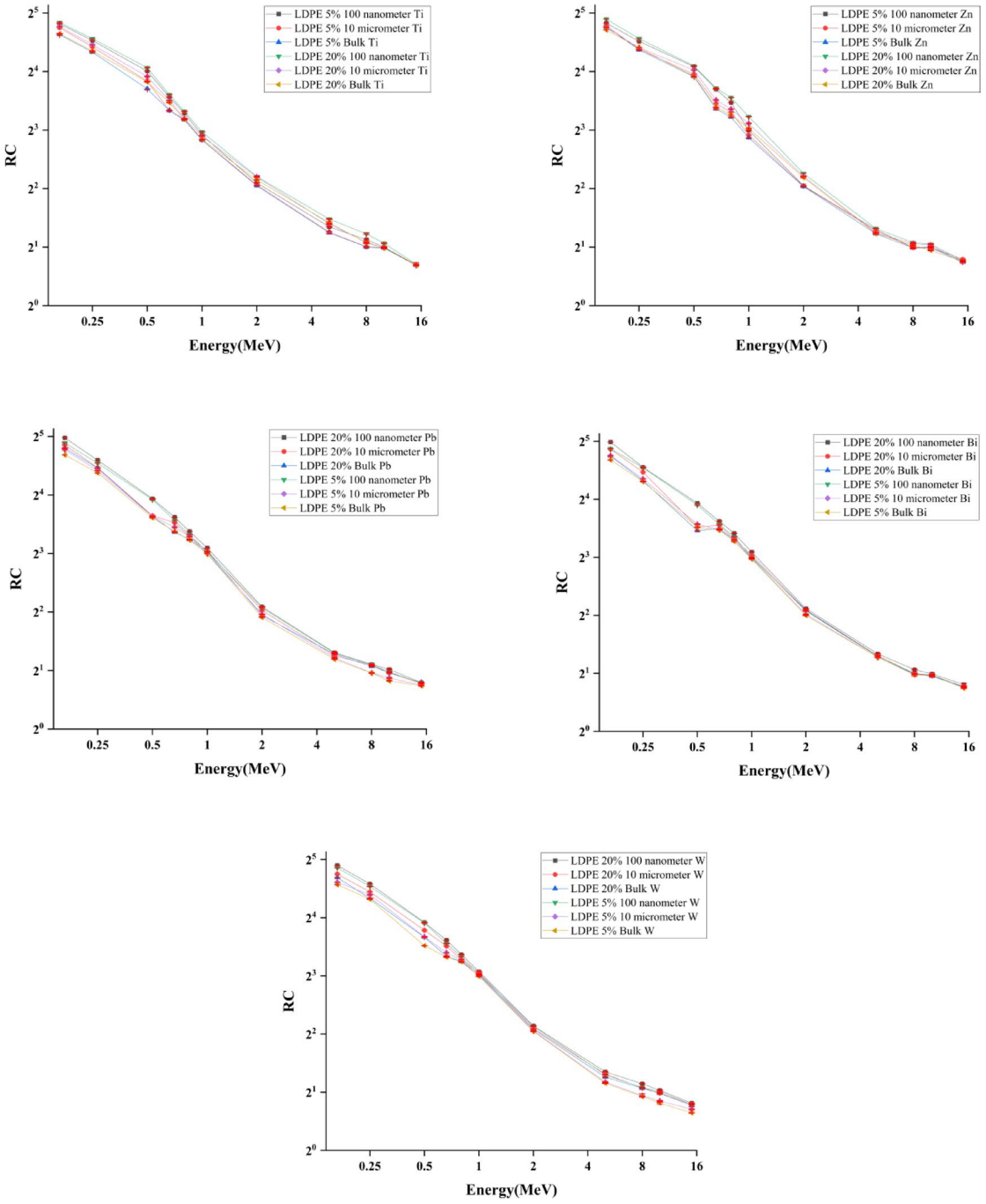

Fig. 3. Variation of the RC versus energy for LDPE doped with two weight percentages (5% and 20%) of W, Zn, Pb, Ti, and Bi particles (the error bars indicate the statistical uncertainty in the results).

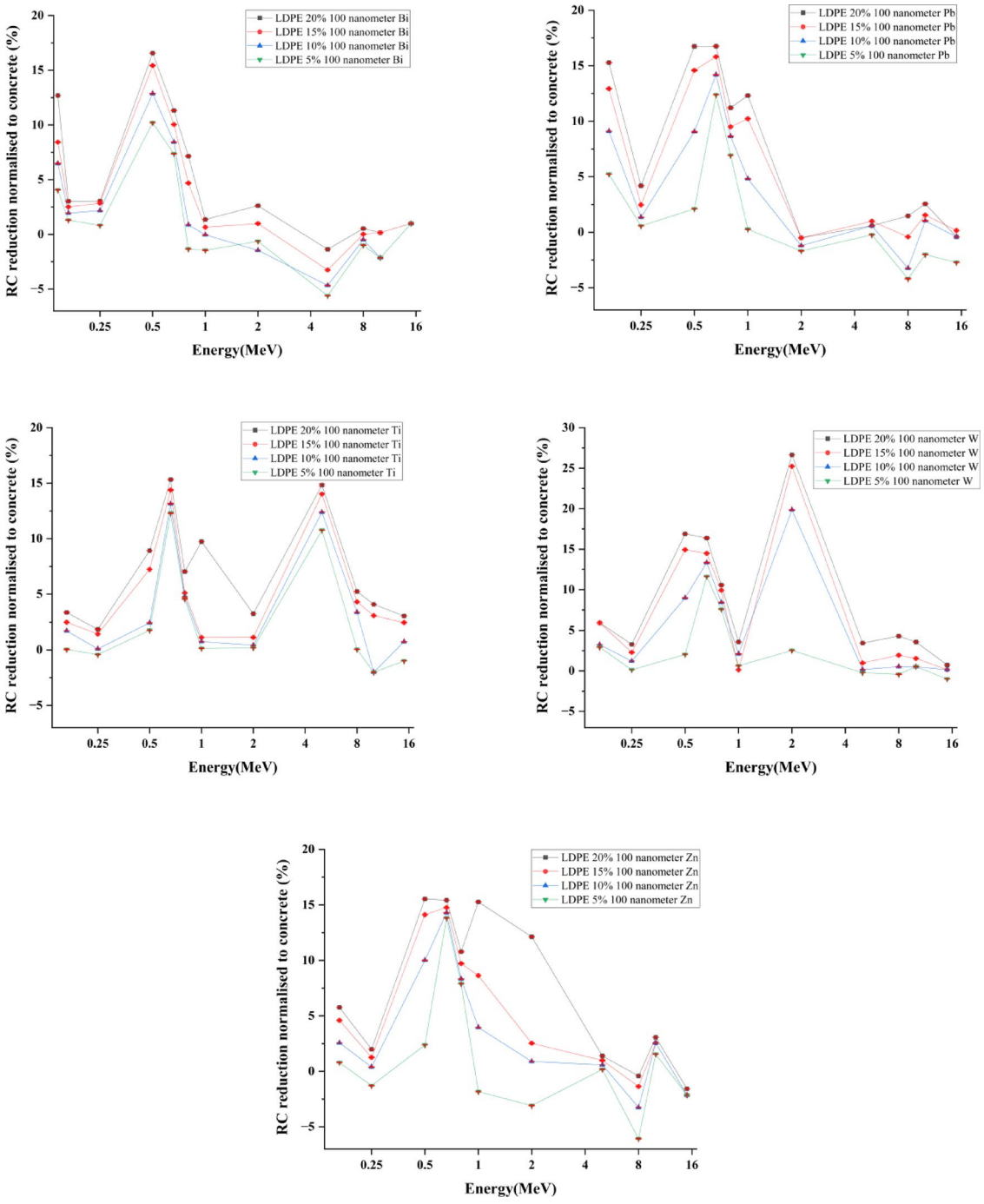

Fig. 4. RC reduction (%) for LDPE composite containing various Pb, W, Bi, Zn, and Ti nanoparticles normalized to ordinary concrete as a function of incident photons energy for 135° reflection angles (the error bars indicate the statistical uncertainty in the results).

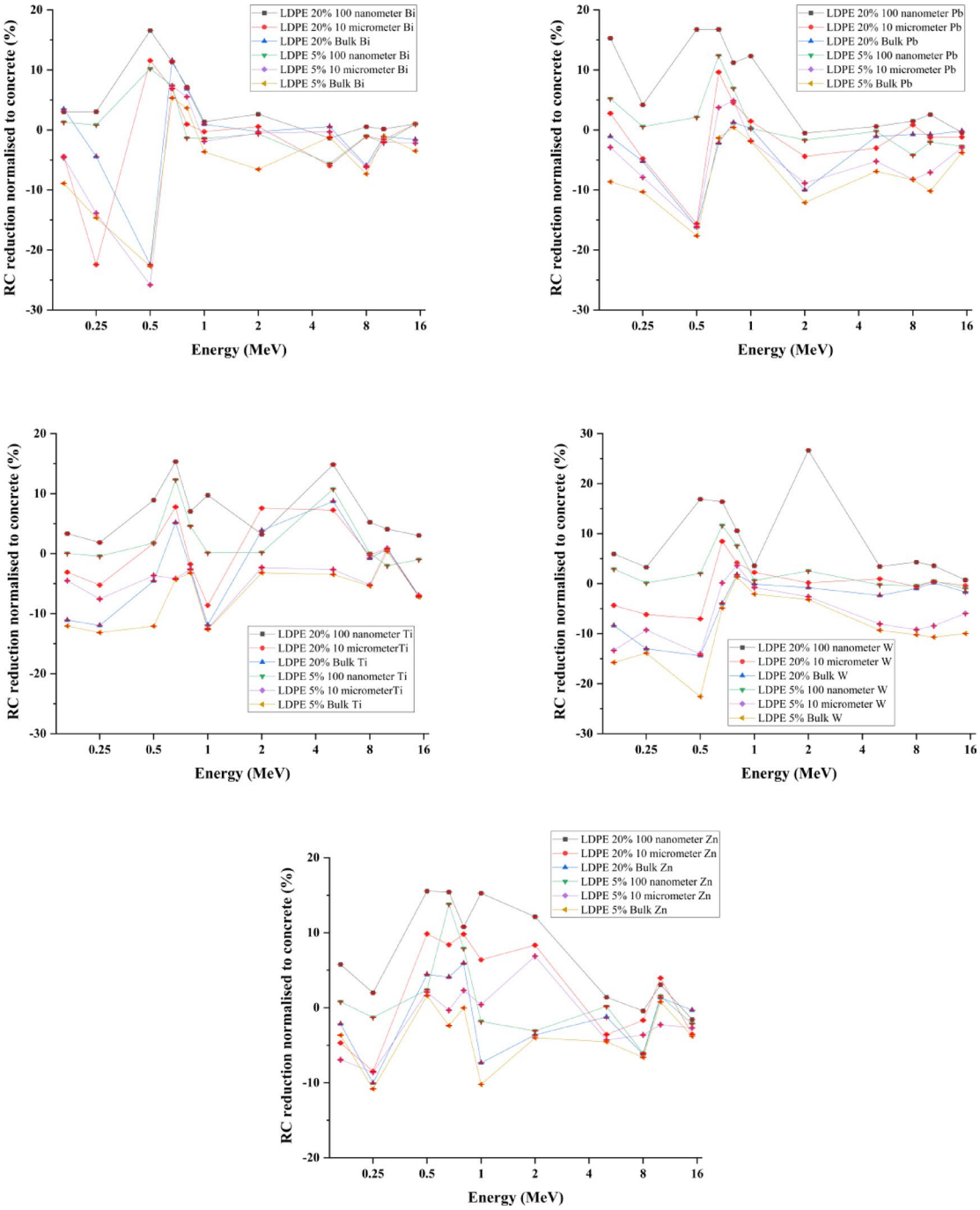

Fig. 5. RC reduction (%) for LDPE containing Pb, W, Bi, Zn, and Ti particles normalized to ordinary concrete as a function of incident photons energy for 135° reflection angles (the error bars indicate the statistical uncertainty in the results).

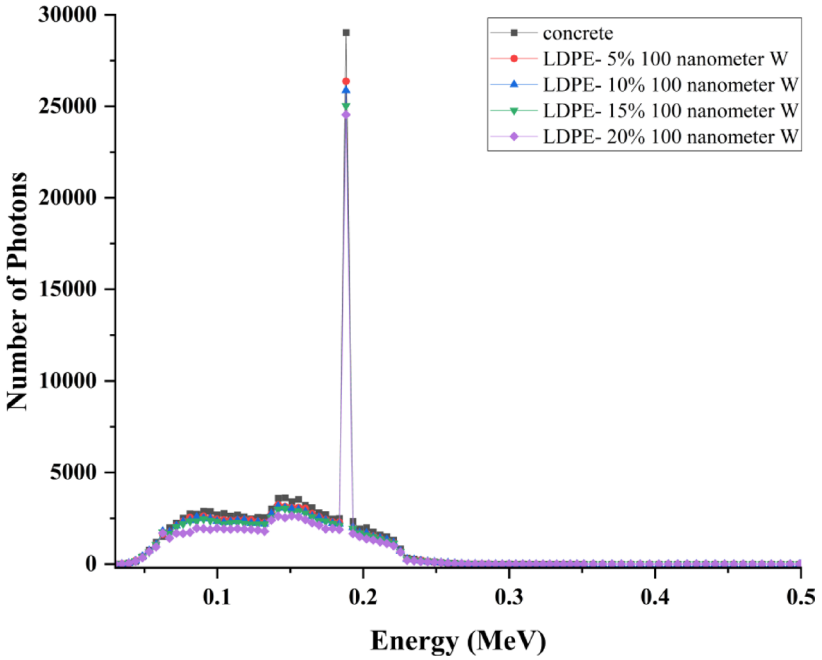

Fig. 6. The spectra of backscattered gamma-rays for LDPE containing various wt% of W nanoparticles at reflection angle of 135° and 0.5 MeV incident photon energy.

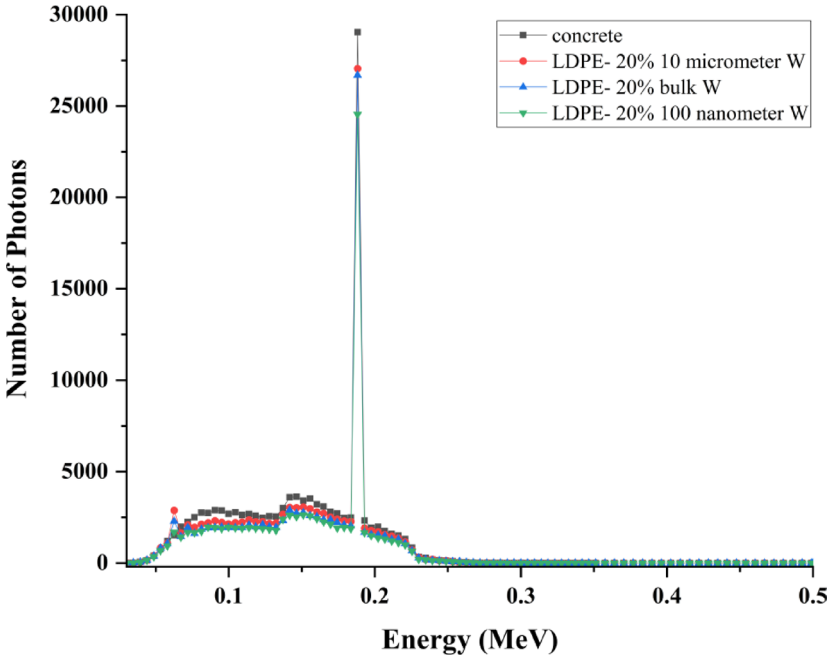

Fig. 7. The spectra of backscattered gamma-rays for LDPE doped with 20 wt% of W particles at reflection angle of 135° and incident photon energy of 0.5 MeV.

Data availability

All data generated or analyzed during this study are included in this published article.

Received: 10 April 2025; Accepted: 17 July 2025
Published online: 14 August 2025

References

1. Sahani, R. M. & Dixit, A. A comprehensive review on zinc oxide bulk and nano-structured materials for ionizing radiation detection and measurement applications. *Mater. Sci. Semicond. Process.* **151**, 107040 (2022).
2. Zhang, H. & Lin, S. Research progress with membrane shielding materials for electromagnetic/radiation contamination. *Membranes* **13**(3), 315 (2023).
3. Hoang, S. M., Yoo, S. H. & Sun, G. M. Experimental validation of the back scattering gamma-ray spectra with the monte carlo code. *Nucl. Eng. Technol.* **43**(1), 13–18 (2011).
4. Mesbahi, A., Azarpeyvand, A.-A. & Shirazi, A. Photoneutron production and backscattering in high density concretes used for radiation therapy shielding. *Ann. Nucl. Energy* **38**(12), 2752–2756 (2011).
5. Kennedy, E. V., Iball, G. R. & Brettle, D. S. Investigation into the effects of lead shielding for fetal dose reduction in CT pulmonary angiography. *Br. J. Radiol.* **80**(956), 631–638 (2007).
6. Alipoor, M., Eshghi, M. & Sever, R. Monte Carlo simulation of gamma and neutron shielding with high-performance ultra-heavy cement composite. *J. Med. Phys.* **49**(4), 661–672 (2024).
7. Aydın, A. Energy distributions of multiple backscattered photons in materials. *Nucl. Sci. Tech.* **29**(2), 23 (2018).
8. Sabharwal, A. D. et al. Albedo factors of 279, 320, 511 and 662 keV backscattered gamma photons. *Radiat. Eff. Defects Solids* **166**(6), 451–458 (2011).
9. Sabharwal, A. D., Singh, B. & Sandhu, B. S. Investigations of multiple backscattering and albedos of 1.12MeV gamma photons in elements and alloys. *Nucl. Instrum. Methods Phys. Res. Sect. B Beam Interact. Mater. At.* **267**(1), 151–156 (2009).
10. Berger, M. J. & Raso, D. J. Monte Carlo calculations of gamma-ray backscattering. *Radiat. Res.* **12**(1), 20–37 (1960).
11. Chalamalla, I. et al. Experiment and Monte Carlo simulation of gamma-ray backscattering from materials for nondestructive testing. *J. Radioanal. Nucl. Chem.* **333**(11), 6033–6037 (2024).
12. Almurayshid, M. et al. Development of new lead-free composite materials as potential radiation shields. *Materials* **14**(17), 4957 (2021).
13. Kaur, T., Sharma, J. & Singh, T. Experimental measurement of effective atomic numbers and albedo factors for some alloys using the backscattering technique. *Appl. Radiat. Isot.* **158**, 109065 (2020).
14. Coakley, J. A. Reflectance and albedo, surface. In *Encyclopedia of Atmospheric Sciences* (ed. Holton, J. R.) 1914–1923 (Academic Press, 2003).
15. Chilton, A. B. & Huddleston, C. M. A semiempirical formula for differential dose albedo for gamma rays on concrete*. *Nucl. Sci. Eng.* **17**(3), 419–424 (1963).
16. Al-Affan, I. A., Qutub, M. A. & Hugtenburg, R. P. Monte Carlo simulation of photons backscattering from various thicknesses of lead layered over concrete for energies 0.25–20 MeV using FLUKA code. *Sci. Rep.* **11**(1), 18362 (2021).
17. Qutub, M. A. Z. Photon backscattering for various stainless steel thicknesses from 0.25 to 20 MeV using Monte Carlo simulation FLUKA code. *Radiat. Phys. Chem.* **202**, 110511 (2023).
18. Kassem, S. M. et al. Novel flexible and lead-free gamma radiation shielding nanocomposites based on LDPE/SBR blend and BaWO4/B2O3 heterostructures. *Radiat. Phys. Chem.* **209**, 110953 (2023).
19. AvcioĞLu, S. LDPE matrix composites reinforced with dysprosium-boron containing compounds for radiation shielding applications. *J. Alloy. Compd.* **927**, 166900 (2022).
20. Alshahri, S. et al. LDPE/bismuth oxide nanocomposite: Preparation, characterization and application in x-ray shielding. *Polymers* **13**(18), 3081 (2021).
21. Alavian, H. & Tavakoli-Anbaran, H. Comparative study of mass attenuation coefficients for LDPE/metal oxide composites by Monte Carlo simulations. *Eur. Phys. J. Plus* **135**(1), 82 (2020).
22. Waters, L. S. et al. The MCNPX Monte Carlo radiation transport code. *AIP Conf. Proc.* **896**(1), 81–90 (2007).
23. McKinney, G., *MCNPX User's Manual, Version 2.6.0*. 2008.
24. NCRP, *NCRP Report 151* Structural shielding design and evaluation for megavoltage x-and gamma-ray radiotherapy facilities. *J. Radiol. Protect.*, 2006. **26**(3) 349.
25. Alavian, H. & Tavakoli-Anbaran, H. Study on gamma shielding polymer composites reinforced with different sizes and proportions of tungsten particles using MCNP code. *Prog. Nucl. Energy* **115**, 91–98 (2019).
26. Kim, J. et al. Nano-W dispersed gamma radiation shielding materials. *Adv. Eng. Mater.* **16**(9), 1083–1089 (2014).
27. Azeez, A. B. et al. Replacement of lead by green tungsten-brass composites as a radiation shielding material. *Appl. Mech. Mater.* **679**, 39–44 (2014).

Author contributions

Aryan Nikrah: Investigation, simulation, data curation, writing original draft preparation. Payvand Taherparvar: Conceptualization, methodology, investigation, data curation, writing (review and editing). Alireza Sadremomtaz: Supervision.

Declarations

Competing interests

The authors declare no competing interests.

Additional information

Supplementary Information The online version contains supplementary material available at https://doi.org/10.1038/s41598-025-12542-1.

Correspondence and requests for materials should be addressed to P.T.